IEEE Access
Multidisciplinary | Rapid Review | Open Access Journal

Date of publication xxxx 00, 0000, date of current version xxxx 00, 0000.

Digital Object Identifier 10.1109/ACCESS.2017.Doi Number

Application of SMES Technology in Improving the Performance of a DFIG-WECS Connected to a Weak Grid

A. M. SHIDDIQ YUNUS[1], A. ABU-SIADA[2], (Senior Member, IEEE) , Mohamed I. Mosaad , (Member IEEE)[3], , Hani Albalawi[4,5] (Member IEEE), Mansour Aljohani[3] and JIAN XUN JIN[6], (Senior Member, IEEE)

[1]Energy Conversion Study Program, Mechanical Engineering Department, PoliteknikNegeri Ujung Pandang, Makassar 90245, INDONESIA
[2]Discipline of Electrical and Computer Engineering, Curtin University, WA, 6102, AUSTRALIA
[3] Electrical and Electronic Engineering Technology Department, Yanbu Industrial college, Yanbu Al Sinaiyah, Yanbu 46452, Saudi Arabia
[4] Department of Electrical Engineering, Faculty of Engineering, University of Tabuk, Tabuk, Saudi Arabia
[5] Renewable Energy and Energy Efficiency Center (REEEC), University of Tabuk, Tabuk, Saudi Arabia
[6]School of Electrical Engineering, Tianjin University, Tianjin, 300072 CHINA

Corresponding author: A. M. ShiddiqYunus (e-mail: shiddiq@ poliupg.ac.id), Mohamed I. Mosaad (m_i_mosaad@hotmail.com).

ABSTRACT- Wind Turbine Generator (WTG) has become one of the most popular renewable-based power generation that is broadly connected to electricity grids worldwide. Till the year 2019, the total WTGs installed worldwide reached about 650.8GW. The WTG is interfaced to the electricity grid through power electronic converters with a proper control algorithm to facilitate a smooth power delivery as well as maintaining the system voltage and frequency stability during wind intermittency. However, power grids are usually subjected to load expansion which affects the stiffness of the grid and hence its stability. A weak electricity grid exhibits voltage instability that may affect the performance of WTGs and in some cases may lead to serious damages to the wind turbines and the entire system. In this paper, superconducting magnetic energy storage (SMES) technology based on fuzzy logic controller is implemented to effectively resolve this issue and improve the overall performance of WTGs. Hysteresis current and fuzzy logic-based control system is proposed to control the energy exchange between the SMES coil and the investigated system. Results show the effectiveness of the SMES to improve the overall system performance and along with the fault ride-through capability of the doubly-fed induction generator (DFIG).

INDEX TERMS DFIG, SMES, Low voltage ride through, Wind energy, Weak grid.

I. INTRODUCTION

In the last decade, electric power generation from non-fossil fuel resources has been given much concern by worldwide nations that allocated a significant portion of its budgets to finance and develop renewable energy-based projects. Among renewable energy sources that have been widely deployed is the wind turbine generators (WTGs). As such, improving the performance of wind power system connected to electricity grids has been given much attention by network operators as well as global researchers. The global installation of WTGs has reached about 650.8 GW at the end of 2019, which was slowed down in 2020 due to Covid-19 [1]. In Indonesia, 75 MW WTG-grid connected systems have been installed recently with another 72 MW in progress [2, 3].

Based on [4], doubly-fed induction generator (DFIG) has occupied 50% of the total installed wind energy conversion systems (WECS) which makes it dominating the total installations among the other types of WTGs worldwide. This DFIG domination is due to its advantages which include: easy control of the active and reactive power, grid and generator sides' controllability and ability to function under variable wind speed. DFIG employs power converters of one-third of the rated power which results in a reduction of the total cost when compared with the full-converter systems [5].

In the early stages of WTG installation, the most challenging issue was how to adapt the turbine rotation with the rapid variation of the wind speed [6-8]. In [6], a maximum power point tracking (MPPT) system is used as a control strategy for optimal extraction of wind energy under

This article has been accepted for publication in a future issue of this journal, but has not been fully edited. Content may change prior to final publication. Citation information: DOI 10.1109/ACCESS.2021.3110995, IEEE Access

the irregular variations of the wind speed. The MPPT control strategy has been also adopted for large-scale of WECS [7]. Ref [8] presents strategies for pitch control to overcome the effect of wind speed intermittency. These studies focused on the improvement of the control mechanism of WTGs under wind speed intermittent conditions. Currently, several WTGs are connected to the main electricity grids. Thus grid stiffness and disturbances have become serious problems that directly affect the performance of the WTGs. Previously, disconnecting wind turbines from the electricity grid during disturbance and fault events was permitted to avoid potential consequences to the components of the WECS. However, the global transmission line operators have established strict grid codes that must be complied to maintain the connection of the wind turbines during such events to support the grid and avoid partial or full power blackout. In some cases, without a proper protection scheme, a grid disturbance may lead to the disconnection of the WTGs or result in severe damages to the turbine and converter switches [9].

Due to the day-by-day increase in the loads, electricity grids are becoming less stiff as no more synchronous generator-based power plants are connected to support the grid [10]. This situation will affect the WTG performance, especially when a DFIG is used due to the sensitivity of these generators to the grid characteristics, faults and disturbance events [11].

II. PAPER CONTRIBUTION AND NOVELTY

A weak grid is usually associated with voltage instability [12] that affects the performance of the WTGs connected to the grid and in some cases, may result in serious damages to the mechanical and electrical components of the WTGs. While several studies on the improvement of WTGs control strategies for weak grids can be found in the literature [13–16], all the presented control techniques are only suitable for newly installed WTGs as they call for major changes to the built-in control mechanism and infrastructure of the WTG.

Ref [13] presents the impact of wind speed levels on the performance of a DFIG-based WECS when connected to a weak-grid using small-signal analysis. A control improvement for the grid side converter is introduced [14] to enhance the DFIG performance when connected to a weak grid. In [15], the presented investigation focused on the impact of weak grids on the performance of a large-scale WECS based on voltage sensitivity at the point of common coupling (PCC) however, no solution is proposed. To maintain system stability, Ref [16] proposed an improved low voltage ride through (LVRT) control scheme by either injecting active current or decreasing the phase locked loop (PLL) bandwidth.

For existing systems, a flexible ac transmission system (FACTS) device can be connected to resolve the issue of connecting a WECS to weak grids [17]. Many FACTS devices were employed to improve the performance of WTGs. This includes high-temperature superconductors connected to the converters dc-link, superconducting magnetic energy storage (SMES) unit, unified power flow controllers, static synchronous series compensators and static compensator (STATCOM) [18-22]. These FACTS devices are employed to enhance the fault ride-through (FRT) capability of WTG-DFIGs, smoothen generated power fluctuation and improve the power quality [20-22]. A recent study of suppressing unbalanced grid voltage using coordinated control of permanent magnet synchronous generator (PMSG) and STATCOM has been introduced in [23]. By controlling the virtual negative-sequence output admittance of the PMSG and STATCOM, the grid voltage unbalance can be compensated.

From the above discussion, it can be observed that not much attention was given to simultaneously enhance both the fault ride through of the WECS-DFIG and its dynamic performance when connected to a weak grid.

The main contribution and novelty of this paper is the presentation of a new application for SMES unit to simultaneously improve the dynamic performance of WTG-DFIG connected to a weak grid and improve the FRT of the DFIG. The energy exchange between the SMES coil and the grid is controlled using hysteresis current-fuzzy logic controller.

III. SYSTEM UNDERSTUDY

Fig. 1 illustrates the tested system, which consists of six identical DFIG-based wind turbines, of 6 x1.5 MW capacity. The DFIGs and the grid are connected through a 30 km distribution line, and the SMES unit is linked to the terminal of the DFIGs at a PCC. A generic model of the DFIG is shown in Fig. 2.

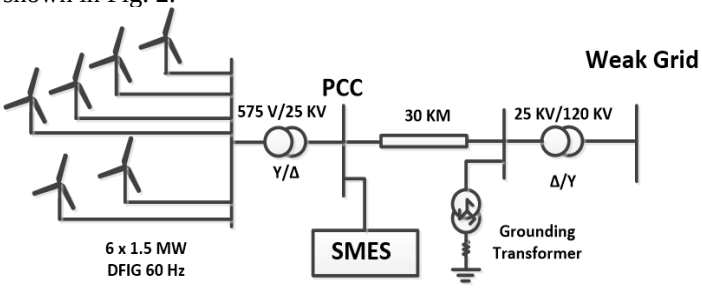

FIGURE 1. Studied System

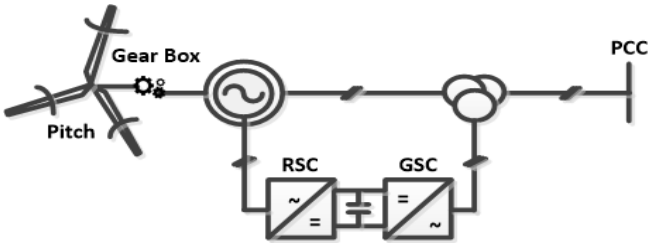

FIGURE 2. Generic model of a DFIG.

The DFIG is interfaced with the grid via two converters. One converter, grid side converter (GSC), is connected to the grid via a coupling transformer while the other one is connected to the rotor and named as the rotor side converter (RSC). The two converters are coupled back-to-back through a dc-link capacitor. The system is designed based on the parameters given in Table 1 to operate normally on an average wind speed of 15 m/s.

This article has been accepted for publication in a future issue of this journal, but has not been fully edited. Content may change prior to final publication. Citation information: DOI 10.1109/ACCESS.2021.3110995, IEEE Access

The proposed SMES unit has been widely used in several applications such as improving the WECS under wind gust conditions [16], power-leveling [18], large-scale accelerator magnet power supply [19], and power smoothing during wind speed variation [20]. SMES is an efficient FACTS device that features large storage energy with high efficiency of about 98% [21]. In addition, it has fast response that makes it applicable for grid-tied WECS to maintain the continuous operation of the generator during faults and disturbance events.

TABLE I
Parameters of Studied System

Parameters of DFIG	
Rated Power	(6 x 1.5 MW) = 9 MW
Stator Voltage	575 V
Operating Frequency	60 Hz
Stator resistances R_s	0.023 pu
Rotor resistance R_r	0.016 pu
Converter Based Value	1000 V
PCC base voltage V_{pcc}	25 kV
Parameters of the distribution line	
R_1, R_0 (Ω/km)	0.1153, 0.413
L_1, L_0 (H/km)	1.05 x 10^{-3} , 3.32 x 10^{-3}
C_1, C_0 (F/km)	11.33 x 10^{-9}, 5.01 x 10^{-9}
Parameters of SMES	
Maximum Rated Capacity	6 MJ
Maximum Rated SC Current	2 kA
Data of The Grid	
Grid Capacity	2500 MVA
Grid Voltage	120 kV
X_0/X_1	3

IV. SMES CONTROLLER

The common layout of the SMES unit is displayed in Fig.3. The unit contains a voltage source converter (VSC) and a dc-dc chopper that interface the SMES coil to the PCC. To facilitate a constant voltage at the PCC, a dc-link capacitor is placed between the VSC and the dc-dc chopper. The chopper controls the energy exchange between the SMES coil and the system. With a proper control algorithm, energy exchange can be conducted rapidly, smoothly and in four-quadrant operational mode.

The SMES control principle can be categorized into voltage or current source converters (VSC and CSC). VSC outperforms the CSC in terms of better self-commutation and reduced implementation cost. The idea behind using SMES unit to enhance the performance of DFIG-WECS has been presented in the literature [21, 22].

In this paper, the proposed control system for the SMES unit employs a VSC. The cost of the switching devices required for the VSC is about 173% less than a CSC of a similar size. Moreover, the VSC features better self-commutation capability and less harmonic generation [24].

The energy stored E in the SMES coil is based on the SMES current ($\boldsymbol{I_{SMES}}$) and the inductance of the coil ($\boldsymbol{L_{SMES}}$); $\boldsymbol{E = \frac{1}{2} I_{SMES}^2 L_{SMES}}$. The exchange of this stored energy with the system through controlling the SMES unit charging and discharging operational modes is the crux of the effective utilization of the SMES in many applications.

The exchange of SMES energy with the system in this paper is controlled by regulating the switching operation of the VSC and the dc-dc chopper using hysteresis current controller (HCC) and fuzzy-logic controller (FLC), respectively as shown in Fig.3.

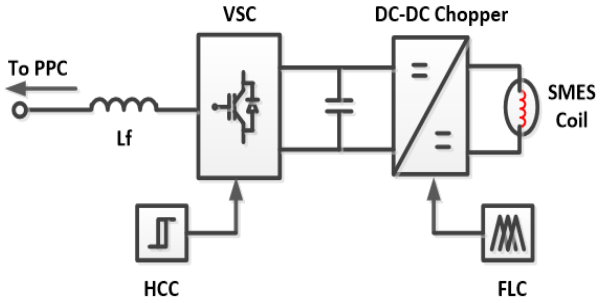

FIGURE 3. Schematic of SMES control configuration.

1- Hysteresis current controller

Several control algorithms were proposed to control the switching operation of VSCs to regulate the voltage across the dc side. Ref. [25] presented a three-level control method for a VSC interfacing a SMES coil with the WECS. However, the complexity of this method makes it infeasible for practical applications. Another method using four proportional-integral (PI) controllers are presented in [26-28]. However, adjustment of the four PI control parameters is a complex task and calls for effective optimization technique.

The concept of HCC can be explained through the VSC-grid equivalent circuit shown in Fig. 4. In this figure, the line currents i_a, i_b and i_c are to be controlled by switching the IGBTs to the positive or negative dc voltage source terminal ($\pm V_{DC}$). The three phase output voltage (V_{abc}) can be converted, for simplicity, to a vector $x(t)$ represented in the stationary frame as $x(t) = x_\alpha(t) + jx_\beta(t)$ where:

$$\begin{bmatrix} x_\alpha \\ x_\beta \end{bmatrix} = \frac{2}{3}\begin{bmatrix} 1 & -\frac{1}{2} & -\frac{1}{2} \\ 0 & \frac{\sqrt{3}}{2} & -\frac{\sqrt{3}}{2} \end{bmatrix}\begin{bmatrix} x_a \\ x_b \\ x_c \end{bmatrix} \quad (1)$$

The terminal voltages can be obtained mathematically as:

$$\begin{aligned} V_a &= S_a * V_{DC} \\ V_b &= S_b * V_{DC} \\ V_c &= S_c * V_{DC} \end{aligned} \quad (2)$$

where S_a, S_b, and S_c are the switching function of each phase.

When S_a, S_b or S_c is connected to $+V_{DC}$, their value in (2) is equal to 1 while it is 0 when the switches are connected to

This article has been accepted for publication in a future issue of this journal, but has not been fully edited. Content may change prior to final publication. Citation information: DOI 10.1109/ACCESS.2021.3110995, IEEE Access

$-V_{DC}$. Thus, the controller purpose is to find the value of those switching functions.

The following state space equations can be derived from Fig. 4:

$$\frac{di_a}{dt} = \frac{1}{3L}[2(v_a - e_a) - (v_b - e_b) - (v_c - e_c)] - \frac{R}{L}i_a$$

$$\frac{di_b}{dt} = \frac{1}{3L}[2(v_b - e_b) - (v_a - e_a) - (v_c - e_c)] - \frac{R}{L}i_b \quad (3)$$

$$\frac{di_c}{dt} = \frac{1}{3L}[2(v_c - e_c) - (v_a - e_a) - (v_b - e_b)] - \frac{R}{L}i_c$$

$$\frac{dI_0}{dt} = \frac{1}{L}(V_n - e_0) - \frac{R}{L}I_0 \quad (4)$$

Using (1), the vector representation of (3) can be written as:

Where e_0 is the counter-emf voltage and I_0 is the output current.

If I^* is the current reference or the current command space vector and I_e is the error, therefore:

$$I_e = I^* - I_0 \quad (5)$$

Eq. 4 and 5 can be used to derive the current error vector differential equation as:

$$L\frac{dI_e}{dt} + RI_e = L\frac{dI^*}{dt} + RI^* - (V_n - e_0) \quad (6)$$

Therefore, the current error vector, I_e changes with the circuit time constant (L/R). It also depends on the current command space vector I^* and its derivative dI^*/dt. Furthermore, I_e is also affected by the counter-emf e_0 *and* the output voltage V_n. If R is ignored, the desired output voltage, V_n^* to reach zero current error can be obtained from:

$$V_n^* = e_0 + L\frac{dI^*}{dt} \quad (7)$$

Then the below equation can be obtained from (6) and (7):

$$L\frac{dI_e}{dt} = V_n^* - V_n \quad (8)$$

From the above equations, it can be observed that the zero current error is defined by the counter-emf voltage space vector and the command current vector.

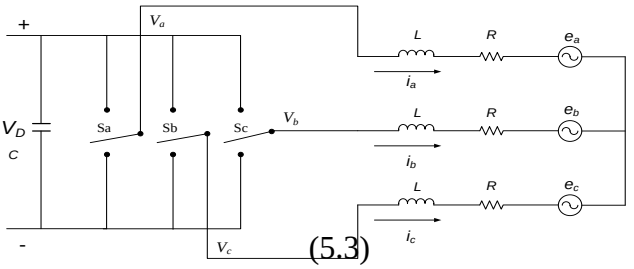

(5.3)

FIGURE 4. **Equivalent schematic diagram of a VSC connected to the grid.**

In this paper, a 3-phase HCC is employed to control the switching operation of the VSC of the SMES unit as demonstrated in Fig. 5. In this technique, three hysteresis bands of width h are specified around the reference 3-phase currents. For any error signal arising by comparing the line and the reference currents, the corresponding inverter leg direction is shifted to the positive or negative terminal by the hysteresis band h. Figs. 6 and 7, respectively, show a typical example of hysteresis current and switching signal.

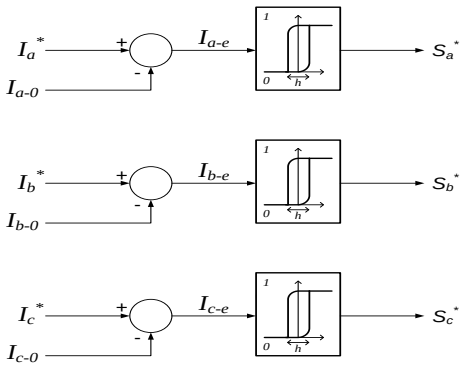

FIGURE 5. **Control of VSC using HCC.**

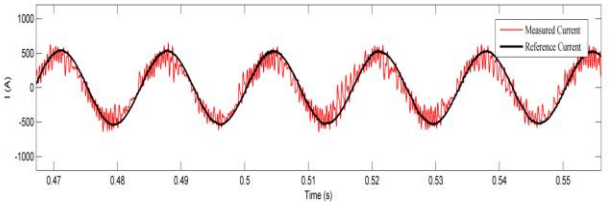

FIGURE 6. **Typical hysteresis current waveform.**

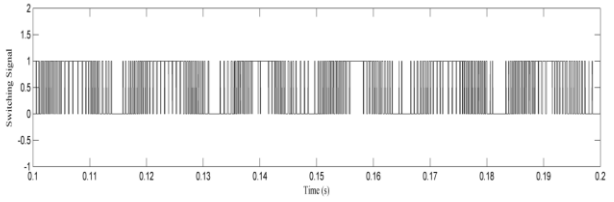

FIGURE 7. **Typical switching VSC signal.**

HCC has been reported to be an effective controller for VSCs because of its simple and easy implementation [21] and hence is employed in this paper as seen in Fig. 8. In this figure, the DFIG terminal voltage (V_S) and the dc-link voltage

This article has been accepted for publication in a future issue of this journal, but has not been fully edited. Content may change prior to final publication. Citation information: DOI 10.1109/ACCESS.2021.3110995, IEEE Access

(V_{DC}) are measured and fed into PI controllers to create two signals in the *dq*-reference frame (I_D and I_Q) that are converted to the *abc*-reference frame and compared with the DFIG line currents. The error signal of the above two currents is used as an input to the HCC. As explained above, the VSC switching pattern is triggered based on the difference between the current error signal and a pre-defined range. This range is updated based on the dc-link voltage and the generator terminal voltage. PLL is used to lessen inter-phases dependency and to keep the switching frequency within acceptable limits [21].

2- Fuzzy-logic controller

The dc-dc chopper is utilized to manage the energy exchange among the system and the SMES coil, by regulating the chopper duty cycle (D) using a FLC. As shown in Fig. 5, a set of fuzzy logic rules are developed based on the deviations of the DFIG generated power (P_G) and the SMES current (I_{SMES}) from their respective nominal values. The output of the FLC is the duty cycle D that is normalized in the range 0 to 1 using a sawtooth signal to control the operation of the dc-dc chopper switches [29, 30].

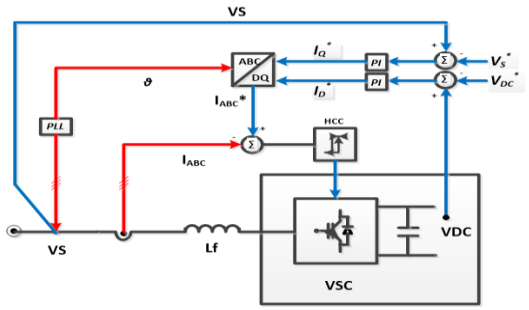

FIGURE 8. **Control of VSC using HCC.**

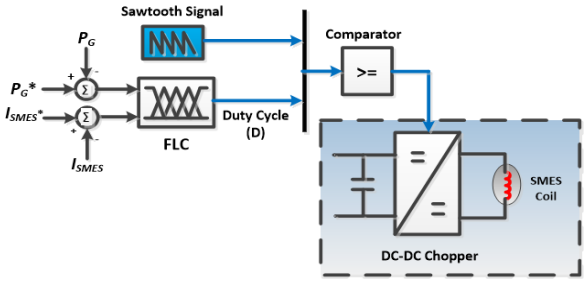

FIGURE 9. **Control of dc-dc Chopper using FLC.**

During normal operation, no energy is exchanged between the system and the SMES coil, therefore a bypass switch is used to short circuit the coil to maintain its stored energy as shown in Fig. 10. Based on the correlation between the coil voltage (V_{SMES}) and the SMES dc-link voltage ($V_{DC,SMES}$) given by (9), the value of D should be 0.5 during normal operating condition.

$$V_{SMES} = (1 - 2D)V_{DC,SMES} \qquad (9)$$

In case of increased grid power as a result of load shedding or additional generation, the FLC acts to regulate the value of D to be in the range 0.5 and 1. This results in a negative voltage across the SMES coil and converts its operation to charging mode. On the other hand, the developed FLC acts to regulate the value of D to be within the range 0 to 0.5 i.e. discharging mode when the system calls for additional energy from the SMES coil. As the SMES coil has always unidirectional current, then the power flow is mainly controlled by controlling the polarity of the voltage across the coil [18-21].

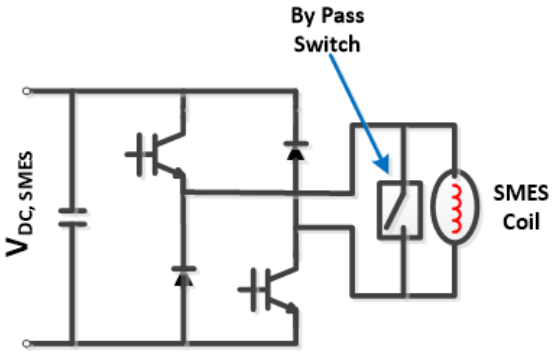

FIGURE 10. **dc-dc Chopper topology.**

V. RESULTS AND DISCUSSION

The application of the SMES unit to improve the performance of a DFIG-based wind energy conversion system connected to a weak grid is elaborated in case study-1. Also, case study-2 is presented to show the effectiveness of the proposed controller in enhancing the FRT capability of the investigated DFIG. Case study-3 investigates the performance of the proposed controller under a 100% voltage drop at the PCC.

A- Case study-1

Assuming a weak grid, the voltage at the grid terminals is expected to exhibit a fluctuation which is assumed in this case study to be within ±30% of the nominal value as shown in Fig 11. The performance of the DFIG under such event is investigated through simulation analysis conducted using Matlab/Simulink software tool.

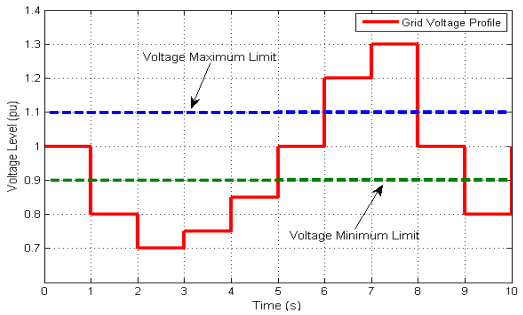

FIGURE 11. Assumed voltage profile at the weak-grid side.

It is obviously clear from Fig. 12(a) that that DFIG generated power is influenced by the assumed scenario for the voltage profile at the grid side. Fluctuation of the generated power is in the range 0.8 pu to 1.3 pu when no control scheme is adopted.

This article has been accepted for publication in a future issue of this journal, but has not been fully edited. Content may change prior to final publication. Citation information: DOI 10.1109/ACCESS.2021.3110995, IEEE Access

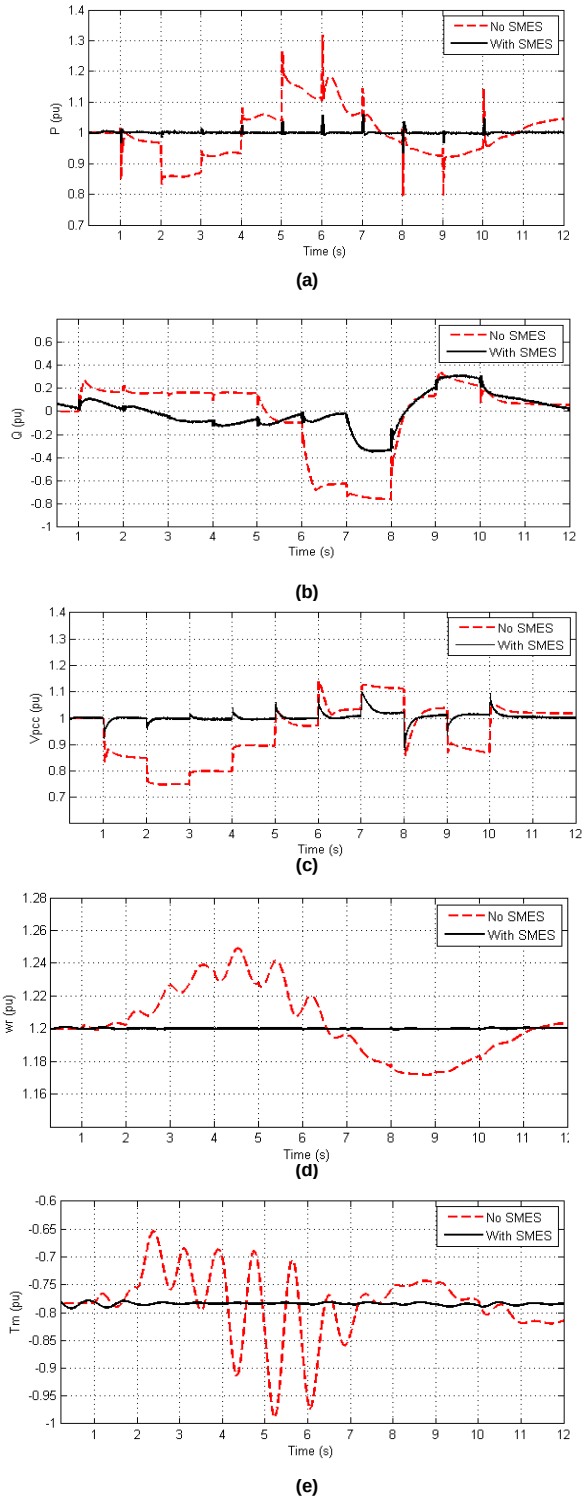

FIGURE 12. DFIG performance during grid voltage variation with and without SMES; (a) DFIG active power; (b) DFIG reactive power; (c) Voltage at PCC; (d) DFIG rotor speed; (e) DFIG electromagnetic torque.

However, with the connection of the proposed SMES unit at the PCC along with the proposed control system, the DFIG generated power is maintained almost constant at the rated value due to the active power modulation managed by the SMES unit. Yet, some spikes can be seen due to the assumed sudden changes in the voltage profile at the grid side.

Without the SMES unit, the DFIG injects or absorbs reactive power to control the voltage at the grid side as shown in Fig. 12(b). This results in a significant fluctuation from -0.8 pu to 0.3 pu in the reactive power at the PCC. By connecting the SMES unit, reactive power compensation is conducted through exchanging the stored energy with the system to reduce the fluctuation in the DFIG reactive power. This can be noticed in Fig. 12(b) in which the reactive power fluctuation exhibits a significant reduction and becomes closer to a unity power factor operational mode.

The voltage profile at the PCC as shown in Fig. 12(c) experiences voltage sags and swells following the grid voltage variation. This may turn on the crowbar protection system to isolate the WTGs if the terminal voltage violates the fault ride through grid codes [20]. When the SMES unit is connected, the voltage at the PCC can be maintained at its nominal level with some spikes regardless the grid voltage variation.

As shown in Fig. 12(d), during grid voltage variation, the generator rotor speed tends to increase during voltage sag and decrease during voltage swell following the variations in the generated active power. With the SMES unit, the generator speed profile is kept constant at its rated level. This is attributed to the active power compensation conducted by the SMES unit which alleviates the compensation by the rotor mechanical shaft. Following the fluctuation in the generator speed, the electromagnetic torque experiences substantial oscillations during the grid voltage variations, but when the SMES unit is connected, the oscillations of the electromagnetic torque are effectively suppressed as shown in Fig. 12(e).

The dc-link voltage plays an important role in maintaining the rated energy transfer to the grid. Therefore, it has to be maintained constant as much as possible [21, 22]. Fig. 13 shows that every time the voltage at the grid side encounters changes, the voltage across the dc-link exhibits large overshooting. The zoomed plots shown in Figs. 13(a)-(c) reveal that with the connection of the SMES unit, the maximum overshooting in the dc voltage is significantly reduced, which facilitates a smooth energy exchange between the SMES unit and the system.

Fig. 14 shows the energy profile of the SMES coil ($0.5LI^2$) during the assumed grid voltage variations shown in Fig. 11. It can be seen that the SMES unit injects or absorbs certain amount of energy to regulate both active and reactive power at the PCC and hence reducing the influence of the weak grid on the performance of the WTG.

B- Case study 2

The role of the SMES unit is not limited to improving the performance of WTGs connected to weak grids but it can also perform other tasks for WTGs connected to stiff grids during fault and disturbance events. In this case study, a stiff grid is assumed to experience a three-phase short circuit fault and the same SMES controller is used to improve the performance of the system under such condition.

This article has been accepted for publication in a future issue of this journal, but has not been fully edited. Content may change prior to final publication. Citation information: DOI 10.1109/ACCESS.2021.3110995, IEEE Access

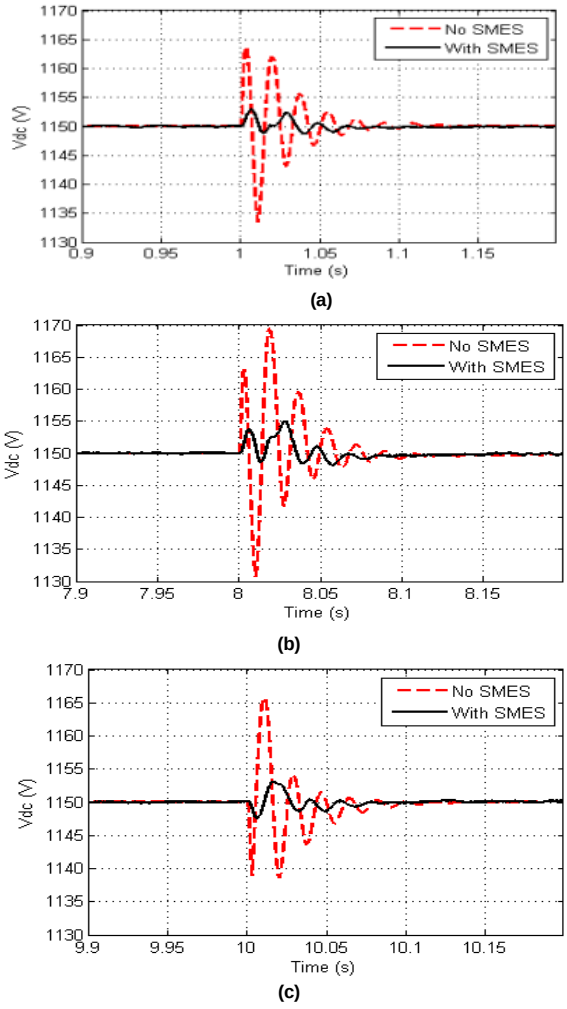

FIGURE 13. DC-link voltage with and without SMES; (a) at t=1s; (b) at t=8s; (c) at t=9s.

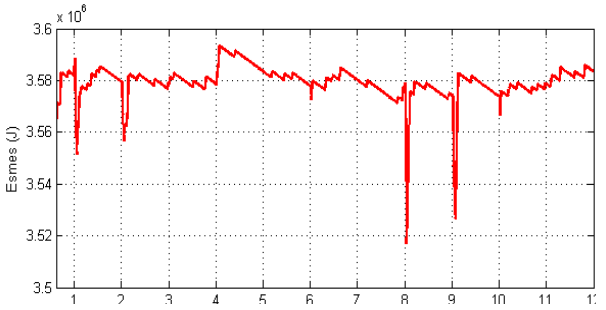

FIGURE 14. SMES energy profile during grid voltage variation.

In this case study, it is assumed a three-phase short circuit fault occurs at the grid side at 0.5s and lasts for 0.25s. The drop in the voltage at the PCC will stimulate the proposed controller to activate the energy exchange between the system and the SMES coil. Due to this fault, the voltage at the PCC experiences a voltage sag of 0.85 pu and reaches a level of only 0.15 pu as can be seen in Fig. 15(a). If this voltage violates the low voltage ride through of some grids' codes such as Spain, the crowbar protection system will be activated and disconnect the WTGs from the grid to avoid potential damages. By employing the proposed SMES unit with the developed controller, the voltage sag at the PCC can be reduced due to the additional reactive power injected by the unit. Accordingly, the PCC voltage level can be brought within the safe margins of Spain grid codes as shown in Fig. 15(a). Without using the SMES unit, the DFIG generated power is dropped to 0.2 pu during this fault as can be seen in Fig. 15(b). This significant reduction may affect system reliability, especially if local loads are connected at the PCC. By connecting the SMES unit, the additional active power released to the system brings the PCC power level to about 0.75 pu as shown in Fig. 15(b).

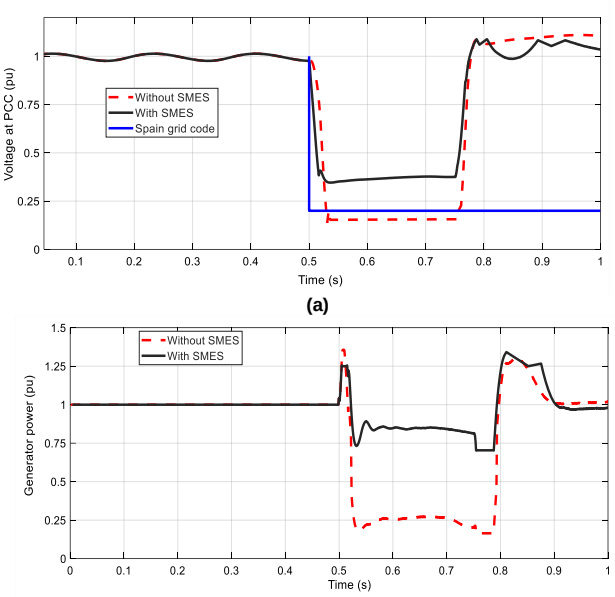

FIGURE 15. DFIG response during three-phase short circuit fault at the grid side with and without SMES; (a) PCC Voltage (b) DFIG active power

C- Case Study-3

In this case, a severe voltage drop of almost 100% for 0.15s is assumed to take place at the PCC. This voltage drop is adopted from the German grid code [30]. As can be seen from Fig. 16, with the use of the proposed SMES unit, the voltage profile at the PCC can be slightly raised up to a level above the minimum allowable voltage level of the German grid code.

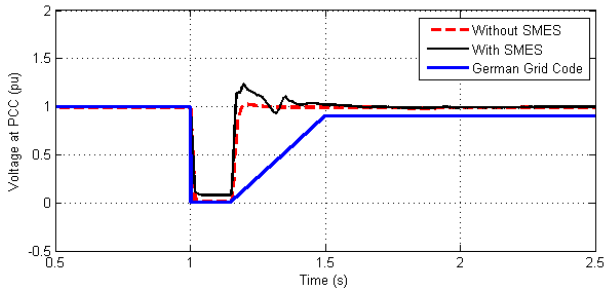

FIGURE 16. Severe voltage drop at the PCC without and with SMES unit.

This article has been accepted for publication in a future issue of this journal, but has not been fully edited. Content may change prior to final publication. Citation information: DOI 10.1109/ACCESS.2021.3110995, IEEE Access

V. CONCLUSION

A weak grid may be due to the expansion of loads which if not properly compensated, will affect the dynamic operation of WTGs connected to the grid. This effect may cause damages or call for the disconnection of the WTGs from the grid. In this paper, the performance of DFIGs connected to a weak grid is investigated without and with a proposed SMES unit. Hysteresis current and fuzzy logic controller is proposed to regulate the energy exchange between the system and the SMES unit. This controller can effectively modulate both active and reactive power at the PCC, smoothly and rapidly in four quadrant operations. Results show that, without the SMES unit, the DFIG experiences substantial fluctuations in the generated power, shaft speed, electromagnetic torque, and the dc-link voltage. With the connection of the SMES unit, the dynamic performance of the DFIGs is maintained within its nominal profile regardless of the voltage variation of the weak grid. The SMES unit can also be used to improve the fault ride-through capability of DFIGs and maintain the connection of WTGs during severe fault events within the grid side. The proposed technique can be adopted for new as well as existing WTGs.

REFERENCES

[1] WWEA, "World wind capacity at 650,8 GW, Corona crisis will slow down markets in 2020, renewables to be core of economic stimulus programmes," 2020. https://wwindea.org/blog/2020/04/16/world-wind-capacity-at-650-gw/ (accessed Sep. 09, 2020).

[2] "Sidrap Wind Farm, Indonesia." https://ecologi.com/projects/sidrap-wind-farm-indonesia (accessed Sep. 10, 2020).

[3] GWEC (Wind Global Council Energy), "Global wind energy report 2018," no. April, pp. 1–61, 2019, [Online]. Available: www.gwec.net.

[4] S. Karad and R. Thakur, "Recent Trends of Control Strategies for Doubly Fed Induction Generator Based Wind Turbine Systems: A Comparative Review," *Arch. Comput. Methods Eng.*, no. 0123456789, 2019, doi: 10.1007/s11831-019-09367-3.

[5] F. Abdou, et al., "Application of STATCOM to improve the LVRT of DFIG during RSC Fire-through Fault", proceeding of AUPEC conference, Bali, Indonesia, September 2012.

[6] A. Ibrahim, E. Solomin, and A. Miroshnichenko, "Control Strategy for Maximum Power Point Tracking of Doubly Fed Induction Motor for Wind Turbine," *Proc. - 2018 Int. Ural Conf. Green Energy, Ural. 2018*, pp. 14–19, 2018, doi: 10.1109/URALCON.2018.8544372.

[7] C. Huang, F. Li, and Z. Jin, "Maximum Power Point Tracking Strategy for Large-Scale Wind Generation Systems Considering Wind Turbine Dynamics," *IEEE Trans. Ind. Electron.*, vol. 62, no. 4, pp. 2530–2539, 2015, doi: 10.1109/TIE.2015.2395384.

[8] M. K. Dhar, M. T. Ahmed, and A. Al, "Wind Turbine using Different control strategies," *2017 IEEE Int. Conf. Power, Control. Signals Instrum. Eng.*, pp. 285–290, 2017.

[9] J. Lopez, E. Gubia, E. Olea, J. Ruiz, and L. Marroyo, "Ride Through of Wind Turbines With Doubly Fed Induction Generator Under Symmetrical Voltage Dips," *IEEE Trans. Ind. Electron.*, vol. 56, no. 10, pp. 4246–4254, Oct. 2009, doi: 10.1109/TIE.2009.2028447.

[10] M. G. Dozein, P. Mancarella, T. K. Saha, and R. Yan, "System strength and weak grids: Fundamentals, challenges, and mitigation strategies," *Australas. Univ. Power Eng. Conf. AUPEC 2018*, no. November, pp. 2019–2021, 2018, doi: 10.1109/AUPEC.2018.8757997.

[11] Mosaad, M.I., Alenany, A., Abu-Siada, "Enhancing the performance of wind energy conversion systems using unified power flow controller" (2020) IET Generation, Transmission and Distribution, 14 (10), pp. 1922-1929.

[12] H. Bindner, *Power Control for Wind Turbines in Weak Grids : Concepts Development*, vol. 1118, no. March. 1999.

[13] W. Jin and Y. Lu, "Stability Analysis and Oscillation Mechanism of the DFIG-Based Wind Power System," *IEEE Access*, vol. 7, pp. 88937–88948, 2019, doi: 10.1109/ACCESS.2019.2926361.

[14] L. J. Cai and I. Erlich, "Doubly Fed Induction Generator Controller Design for the Stable Operation in Weak Grids," *IEEE Trans. Sustain. Energy*, vol. 6, no. 3, pp. 1078–1084, 2015, doi: 10.1109/TSTE.2014.2338492.

[15] X. Tian, H. Tang, Y. Li, Y. Chi, and Y. Su, "Dynamic stability of weak grid connection of large-scale DFIG based on wind turbines," *J. Eng.*, vol. 2017, no. 13, pp. 1092–1097, 2017, doi: 10.1049/joe.2017.0498.

[16] R. Liu, J. Yao, X. Wang, P. Sun, J. Pei, and J. Hu, "Dynamic stability analysis and improved LVRT Schemes of DFIG-Based wind turbines during a symmetrical fault in a weak grid," *IEEE Trans. Power Electron.*, vol. 35, no. 1, pp. 303–318, 2020, doi: 10.1109/TPEL.2019.2911346.

[17] Mohammed I. Mosaad, Ahmed Abu-Siada, Mohamed Elnaggar"Application of Superconductors to Improve the Performance of DFIG-based WECS" IEEE access journal, December 2019, Volume 7, Issue 1, pp103760-103769,DOI: 10.1109/ACCESS.2019.2929261.

[18] A. M. S. Yunus, A. Abu-Siada, M. A. S. Masoum, M. F. El-Naggar, and J. X. Jin, "Enhancement of DFIG LVRT Capability During Extreme Short-Wind Gust Events Using SMES Technology," *IEEE Access*, vol. 8, pp. 47264–47271, 2020, doi: 10.1109/ACCESS.2020.2978909.

[19] A. Abu-Siada, S. Islam, "Application of SMES unit in Improving the Performance of an AC/DC Power System", IEEE Transactions on Sustainable Energy, Vol. 2, No. 2, pp. 109-121, 2011

[20] H. Sato *et al.*, "Application of the SMES for the Large Scale Accelerator Magnet Power Supply," *IEEE Trans. Appl. Supercond.*, vol. 18, no. 2, pp. 779–782, Jun. 2008, doi: 10.1109/TASC.2008.922240.

[21] H. M. Hasanien, "A Set-Membership Affine Projection Algorithm-Based Adaptive-Controlled SMES Units for Wind Farms Output Power Smoothing," IEEE Trans. Sustain. Energy, vol. 5, no. 4, pp. 1226–1233, Oct. 2014, doi: 10.1109/TSTE.2014.2340471.

[22] A. M. S. Yunus, M. A. S. Masoum, and A. Abu-Siada, "Application of SMES to enhance the dynamic performance of DFIG during voltage sag and swell," IEEE Trans. Appl. Supercond., vol. 22, no. 4, 2012, doi: 10.1109/TASC.2012.2191769.

[23] Y. Peng et al., "Coordinated Control Strategy of PMSG and Cascaded H-Bridge STATCOM in Dispersed Wind Farm for Suppressing Unbalanced Grid Voltage," in IEEE Transactions on Sustainable Energy, vol. 12, no. 1, pp. 349-359, Jan. 2021, doi: 10.1109/TSTE.2020.2995457.

[24] M. H. Ali, W. Bin, and R. A. Dougal, "An Overview of SMES Applications in Power and Energy Systems", IEEE Trans. Sustainable Energy, vol. 1, pp. 38-47. Apr. 2010.

[25] A. R. Kim, S. Hyo-Ryong, K. Gyeong-Hun, P. Minwon, Y. In-Keun, Y. Otsuki, J. Tamura, K. Seok-Ho, S. Kideok, and S. Ki-Chul, "Operating Characteristic Analysis of HTS SMES for Frequency Stabilization of Dispersed Power Generation System", IEEE Trans. Appl. Supercond., vol. 20, pp. 1334-1338. Apr. 2010.

[26] S. Jing, T. Yuejin, X. Yajun, R. Li, and L. Jingdong, "SMES Based Excitation System for Doubly-Fed Induction Generator in Wind Power Application", IEEE Trans. Applied Supercond., vol. 21, pp. 1105-1108. Jun. 2011.

[27] S. B. Naderi, M. Negnevitsky, and K. M. Muttaqi, "A Modified DC Chopper for Limiting the Fault Current and Controlling the DC-Link Voltage to Enhance Fault Ride-Through Capability of Doubly-Fed Induction-Generator-Based Wind Turbine," IEEE Trans. Ind. Appl., vol. 55, no. 2, pp. 2021–2032, 2019, doi: 10.1109/TIA.2018.2877400.

[28] A. M. Shiddiq Yunus, M. Saini, A. Abu-Siada, and M. A. S. Masoum, "Impact of SMES unit on dc-link voltage of DFIG during various types and level of faults," Prz. Elektrotechniczny, vol. 95, no. 8, 2019, doi: 10.15199/48.2019.08.27.

[29] A. M. Shiddiq Yunus, A. Abu-Siada, M. A. S. Masoum, "Improving Dynamic Performance of Wind Energy Conversion System using

Fuzzy-Based Hysteresis Current Controlled SMES", IET Power Electronic, Vol. 5, No. 8, pp. 1305-1314, November 2012.

[30] H. Ali, P. Minwon, Y. In-Keun, T. Murata, and J. Tamura, "Improvement of Wind-Generator Stability by Fuzzy-Logic-Controlled SMES", IEEE Trans. Ind. Appl., vol. 45, pp. 1045-1051. May 2009.